

# Magnetism in two-dimensional van der Waals materials

Kenneth S. Burch<sup>1</sup>, David Mandrus<sup>2,3</sup> & Je-Geun Park<sup>4,5\*</sup>

The discovery of materials has often introduced new physical paradigms and enabled the development of novel devices. Two-dimensional magnetism, which is associated with strong intrinsic spin fluctuations, has long been the focus of fundamental questions in condensed matter physics regarding our understanding and control of new phases. Here we discuss magnetic van der Waals materials: two-dimensional atomic crystals that contain magnetic elements and thus exhibit intrinsic magnetic properties. These cleavable materials provide the ideal platform for exploring magnetism in the two-dimensional limit, where new physical phenomena are expected, and represent a substantial shift in our ability to control and investigate nanoscale phases. We present the theoretical background and motivation for investigating this class of crystals, describe the material landscape and the current experimental status of measurement techniques as well as devices, and discuss promising future directions for the study of magnetic van der Waals materials.

Magnetism in two dimensions has long been at the heart of numerous theoretical<sup>1–6</sup>, experimental<sup>7–10</sup> and technological advances<sup>7</sup>, such as the study of topology, the fluctuation-driven generation of new phases and the electrical manipulation and detection of spin. A particularly promising aspect of two-dimensional (2D) magnetism is the ability to rapidly fabricate various 2D heterostructures with engineered levels of strain, chemistry, optical and electrical properties<sup>11–15</sup>. Just as graphene and transition-metal dichalcogenides revolutionized condensed matter and materials engineering, the introduction of a new class of 2D atomic crystals, magnetic van der Waals (vdW) materials<sup>11</sup>, is expected to open up a wide range of possibilities for applications and fundamental research<sup>11,16</sup>. These materials offer a new means to study 2D magnetism, where spin fluctuations are expected to be strongly enhanced<sup>17–19</sup>. Indeed, the wide flexibility of 2D atomic crystals with different elements and structures suggests straightforward tuning of the magnetic anisotropy, which is crucial for reducing or strengthening spin fluctuations and thus various forms of order<sup>5–10,17,19,20</sup>.

The field of magnetic 2D atomic crystals is advancing rapidly<sup>11,18</sup>, with numerous demonstrations of new systems in which 2D magnetism is realized by using only adhesive tape, chemical vapour deposition or molecular beam epitaxy, as was first achieved in graphene. In just the past two years, several notable examples of magnetic order have been observed in single atomic layers of FePS<sub>3</sub><sup>21,22</sup>, CrI<sub>3</sub><sup>23</sup>, Cr<sub>2</sub>Ge<sub>2</sub>Te<sub>3</sub><sup>20</sup>, VSe<sub>2</sub><sup>24</sup> and MnSe<sub>2</sub><sup>25</sup>. This review aims to highlight some of the recent advances in this area and serve as a guide to some of the enormous opportunities provided by the arrival of magnetic vdW materials (see Fig. 1). These opportunities include the thorough examination of well-established theories, such as the Ising transition<sup>3</sup>, the Berezinskii–Kosterlitz–Thouless (BKT) transition of the XY model<sup>4,5</sup> and the Mermin–Wagner theorem<sup>6</sup>. They also include the control and manipulation of magnetic states through coupling to external perturbations such as strain, light, gating, proximity and moiré patterns. In addition, further exotic quantum phases are expected to be revealed in these materials and their heterostructures, including the quantum Hall effect, quantum spin Hall effect, quantum spin liquids and the fractionalization of quasiparticles.

As an example, one can envision thorough experimental investigations of the widely used Mermin–Wagner theorem, which is a rare

example of an exact result in many-body physics. The theorem is often misunderstood to imply that any order in two dimensions is theoretically excluded. Strictly speaking, however, such order is only ruled out for continuous rotational symmetries and short-range interactions. This is mainly due to the enhanced fluctuations in two dimensions, which make symmetry-breaking order unsustainable. However, by gapping the low-energy modes through the introduction of anisotropy, order could be established by providing stabilization of long-range correlations in two dimensions, which is similar to the presence of a magnetically ordered state in the 2D Ising model<sup>20,23</sup>. Given the ease with which anisotropy can be introduced into magnetic systems (for example, via spin–orbit coupling or lattice distortions), we expect to see many more 2D magnetic vdW materials hosting magnetically ordered phases. Moreover, the presence of the intrinsically enhanced and potentially novel fluctuations can produce other types of order that may be useful for producing new types of superconductor<sup>1</sup> and platforms for topological quantum computation<sup>2</sup>.

Another interesting phenomenon observed in 2D magnetic vdW systems is the XY-type interaction. Berezinskii, Kosterlitz and Thouless<sup>4,5</sup> demonstrated in their seminal works that a new type of topological order can emerge that involves the creation of vortex–antivortex pairs. These topological objects are defined by their winding number and can create an ordered state by forming bound pairs of opposite winding numbers. A generalization of this idea is the skyrmion, which is found in certain magnetic systems without inversion symmetry<sup>26</sup>. Interestingly, order can also be suppressed by further enhancing the degeneracy of the ground state and the associated strong spin fluctuations. When these spin fluctuations become dominant, they can mediate the formation of otherwise hidden quantum phases. The arrival of 2D magnetic vdW materials opens up exciting opportunities for studying the emergence of such strong fluctuations and their role in creating novel phases, as well as for understanding new phenomena in the 2D limit. Moreover, because 2D materials do not require lattice matching, a wide range of material combinations become possible (for example, moiré folding of the Brillouin zone<sup>14</sup> or strain-induced effective fields<sup>12</sup>). Although the possibilities are endless, in this article we focus on those that we expect will lead to the biggest potential payoffs in the near future in relation to new physical phenomena and devices.

<sup>1</sup>Physics Department, Boston College, Boston, MA, USA. <sup>2</sup>Department of Materials Science and Engineering, University of Tennessee, Knoxville, TN, USA. <sup>3</sup>Materials Science and Technology Division, Oak Ridge National Laboratory, Oak Ridge, TN, USA. <sup>4</sup>Center for Correlated Electron Systems, Institute for Basic Science, Seoul, South Korea. <sup>5</sup>Department of Physics and Astronomy, Seoul National University, Seoul, South Korea. \*e-mail: jgspark10@snu.ac.kr

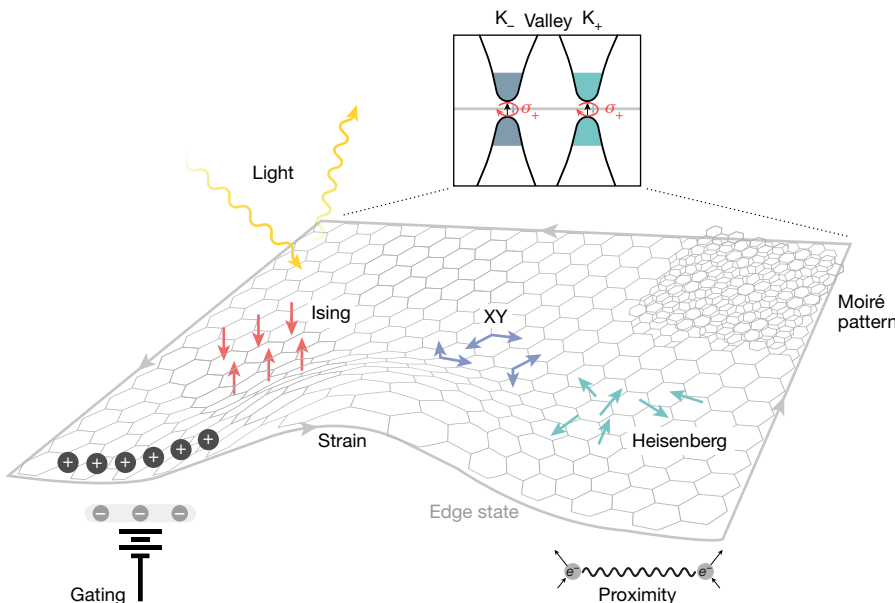


**Fig. 1 | Physical phenomena that can be studied with magnetic vdW materials.** 2D magnetic vdW materials are an ideal platform for investigating how the Hamiltonians of the fundamental magnetism models (the Ising, XY and Heisenberg models; magnetic moments indicated by the red, purple and cyan arrows, respectively) behave in the 2D limit. In addition, the magnetic ground states of these materials could be controlled

by external perturbations, such as gating and strain, or via proximity effects and moiré patterns. Because of the intrinsic properties of their honeycomb lattice, there is also a possibility of light–matter interactions through valley coupling of  $K_-$  and  $K_+$  points in the momentum space and the edge states (grey arrows).

## Material landscape

Most of the magnetic vdW materials are layered, cleavable transition-metal chalcogenides and halides and typically have a layer of metal ions sandwiched between layers of chalcogens or halides. As with other vdW materials, the easy cleavage and lack of dangling bonds allow the creation of nearly perfect surfaces and interfaces, regardless of lattice matching (size or symmetry), providing a vast range of possibilities for such heterostructures<sup>14,27</sup>. These systems have diverse magnetic and electronic properties and include ferromagnetic semiconductors, such as  $Cr_2(Si,Ge)_2Te_6$ <sup>28,29</sup> and  $MSe_2$  ( $M = V, Mn$ )<sup>24,25</sup>, itinerant ferromagnets (FMs), such as  $Fe_3GeTe_2$ <sup>30</sup>, and insulating antiferromagnets (AFMs), such as  $MPX_3$  materials ( $M = \text{transition metal, } X = \text{S or Se}$ )<sup>21,22,31</sup>. There are also materials with strong bond-dependent interactions, such as  $\alpha$ - $RuCl_3$ <sup>32,33</sup>. The spin Hamiltonian and magneto-crystalline anisotropy vary widely from material to material, and they can be tuned through chemical doping, strain or proximity effects. In the near future, we envision efforts focused on developing various thin films via chemical vapour deposition and molecular beam epitaxy<sup>24,25</sup>, as well as new materials with the super-exchange interactions, the spin-orbit interaction and the resulting anisotropy tuned by doping of the non-magnetic atom<sup>34</sup>.

## Optical probes of magnetism

A key challenge is detecting the long-range order, domains and associated magnetic fluctuations. Standard techniques (for example, superconducting quantum interference device (SQUID) magnetometry and neutron scattering) used for bulk crystals, large-area thin films and nanoparticles in solution are unlikely to be successful in magnetic vdW materials, which have small volumes<sup>7</sup>. To evaluate the utility of optical techniques, we consider the energy shifts in the band structure of magnetically ordered materials (Fig. 2a). Specifically, the energy splitting of the spin-up and spin-down states that are associated with the moment is proportional to the strength and sign of the magnetic exchange as well as the magnetization. Assuming that spin-orbit coupling is present, circularly polarized ( $\hat{\sigma}^\pm$ ) light will cause a transition from a particular spin state. This is most easily detected by measuring the circular dichroism in the absorption or reflection, that is, the magneto-circular dichroism (MCD)<sup>35</sup>. Alternatively, one can use the

fact that polarized light ( $\hat{x}, \hat{y}$ ) is a sum of circular polarizations with different phases,  $\hat{x}/\hat{y} = \hat{\sigma}^+ \pm i\hat{\sigma}^-$ . Thus, upon transmission (Faraday effect) or reflection (Kerr effect), linearly polarized light will become elliptical, with the change in the polarization angle being proportional to the magnetization (assuming small angles and no magneto-elastic coupling-induced anisotropy). MCD is thus an important complement to Kerr rotation and magnetization studies, as it is only sensitive to time-reversal-symmetry breaking and generally immune to structural anisotropy. Nonetheless, we note that for both Kerr and MCD the direction and size of the magnetization probed depends sensitively on the wavelength, interference, film thickness and setup<sup>8,36</sup>.

Studies of Kerr rotation versus the applied magnetic field produced the first evidence of order in thin layers of  $Cr_2Ge_2Te_6$ <sup>33</sup> and  $CrI_3$ <sup>20</sup> (see Fig. 2b). In  $CrI_3$  the bilayer system showed zero out-of-plane magnetization up to a critical value of the magnetic field, whereas all other examined materials generally exhibited the hysteresis expected from a ferromagnet. This was interpreted as evidence for an antiferromagnetic configuration between the layers. Although one could expect this to indicate a change in the easy axis of the bilayer system, more recent MCD<sup>37</sup> and tunnelling<sup>38–40</sup> results have confirmed the initial interpretation. We anticipate that a number of more advanced optical approaches will soon be employed. For example, as achieved in magnetic semiconductors<sup>35,41</sup> spectroscopic MCD could measure the strength and sign of the exchange as well as the bands relevant to the magnetic order (Fig. 2a). Furthermore, by applying an a.c. magnetic field, one can measure the susceptibility<sup>9</sup>. This a.c.–Kerr technique, which was first applied to thin films, could be used to measure the Néel temperature and provide insights into low-energy fluctuations, moment size and magnetic frustration.

Alternatively, inelastic light scattering provides access to the energy, symmetry and statistics of lattice, electronic and magnetic excitations in nanomaterials. These techniques rely on the modulation of the optical constants by the fluctuations of some operator. The mixing of such modulations with the optical field produces a response in the sum (anti-Stokes) or difference (Stokes) frequency that results from the creation (annihilation) of an excitation. If the operator is the lattice displacement, the fluctuations are phonons. Via spin-orbit coupling we can also expect coupling to magnetic terms that allow the measurement of various magnetic excitations, including fluctuations of the magnetic energy

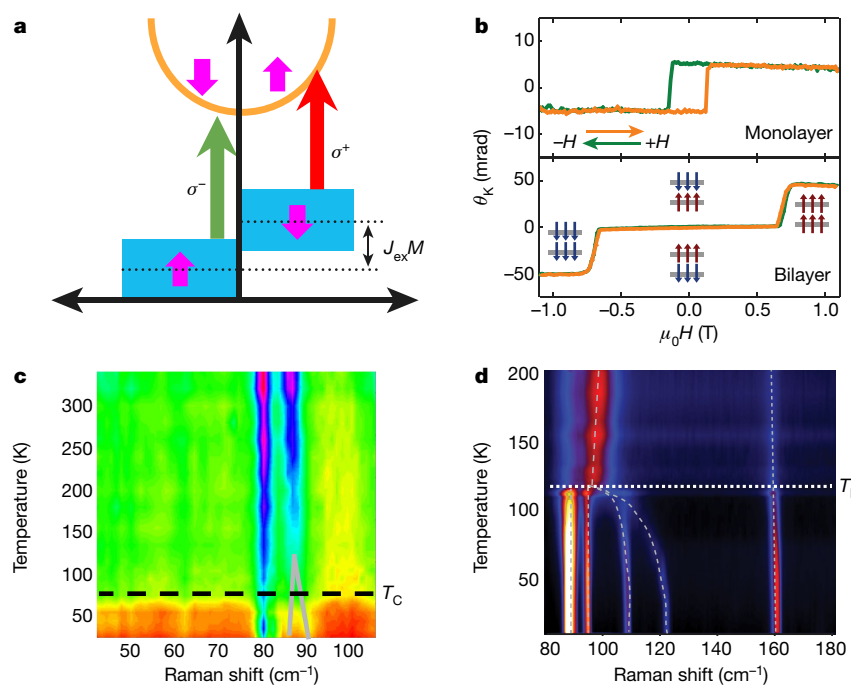


**Fig. 2 | Optical probes of magnetism in two dimensions.** **a**, Density of states for spin-up and spin-down electrons with possible optical transitions for left (green arrows;  $\sigma^-$ ) and right (red arrows;  $\sigma^+$ ) circularly polarized light, respectively. The band is split by the magnetic exchange ( $J_{\text{ex}}$ ) and the net magnetization ( $M$ ), allowing one to measure the magnetization from the resulting circular dichroism in the absorption or reflection and from the rotation of the light polarization upon reflection (Kerr effect) or transmission (Faraday effect). **b**, Polar Kerr rotation angle  $\theta_K$  versus a magnetic field  $\mu_0 H$  applied along the  $c$  axis for single-layer (top) and bilayer (bottom) CrI<sub>3</sub><sup>20</sup> ( $H$ , magnetic field strength;  $\mu_0$ , magnetic constant). The single-layer hysteresis loop is consistent with FM order, whereas the bilayer reveals a metamagnetic transition, consistent with AFM order between layers. The blue and brown

arrows in the bottom graph show the direction of the moments in the layers (grey lines). Image reprinted with permission from ref.<sup>20</sup>, Springer Nature Limited. **c, d**, Raman shift versus temperature for Cr<sub>2</sub>Ge<sub>2</sub>Te<sub>6</sub> (**c**; image reprinted from ref.<sup>29</sup>) and single-layer FePS<sub>3</sub> (**d**; image reprinted with permission from ref.<sup>21</sup>). Copyright 2016 American Chemical Society, with the ordering (Curie/Néel) temperature shown by the horizontal dashed lines. Both figures reveal changes in the phonons due to magnetic order; for example, degeneracy lifting in Cr<sub>2</sub>Ge<sub>2</sub>Te<sub>6</sub> (grey lines) and zone folding (indicated by the splitting of the low-energy peaks) for FePS<sub>3</sub>. The broad background in **c** results from quasi-elastic scattering due to magnetic thermal fluctuations. The colour scales indicate the intensity (high intensity, red; low intensity, green (**c**) and high intensity, red; low intensity, black (**d**)).

density (that is, quasi-elastic scattering), acoustic and optical magnons, and spinons (fractional magnons expected in frustrated systems). One example is the Raman scattering from Cr<sub>2</sub>Ge<sub>2</sub>Te<sub>6</sub>, shown in Fig. 2c. Here a broad background is seen for all temperatures above the Curie temperature ( $T_C$ ), which results from thermal magnetic fluctuations<sup>29</sup>. Additionally, magneto-elastic coupling splits the optical modes for temperatures above  $T_C$  owing to the presence of short-range order.

Raman spectroscopy also provided the first evidence for long-range order in a single-layer magnetic vdW material<sup>21,22</sup>. Specifically, single-layer FePS<sub>3</sub> at high temperatures showed a broad feature at low energies (see Fig. 2d). Upon cooling below the Néel temperature ( $T_N$ ), the broad feature splits into four modes. This results from zone-folding due to the presence of the zig-zag antiferromagnetic order and from the zone-boundary modes becoming Raman-active (that is, they are folded to the zone centre)<sup>21,22</sup>. Raman spectroscopy also first revealed the strength of the magnetic exchange in a magnetic vdW material via measurements of the two-magnon joint density of states<sup>42</sup>. For uncovering novel topology, Raman spectroscopy can also measure the non-trivial statistics associated with fractional spin excitations<sup>43</sup>. Lastly, Brillouin light scattering has been employed in thin films and devices to image the spin injection of electrons and the magnon chemical potential<sup>44,45</sup>. Considering that Brillouin light scattering has been used to measure acoustic modes in graphene<sup>46</sup>, we anticipate that it will soon reveal the strength of the exchange, anisotropy and spin-injection efficiency in magnetic vdW materials and devices.

### Initial devices and electrical probes

The surprising AFM state of the CrI<sub>3</sub> bilayer<sup>20</sup> was soon confirmed via tunnelling across heterostructures of graphene(ite)/CrI<sub>3</sub>/graphene/hBN (hexagonal boron nitride) (Fig. 3a)<sup>38–40</sup>. Consistent with earlier studies

of artificial multilayers<sup>45,46</sup>, tunnelling was suppressed in the AFM configuration. Tuning the out-of-plane magnetic field produces a large and sudden increase in tunnelling, with switching from an AFM to an FM configuration (see Fig. 3a). This can be understood by considering CrI<sub>3</sub> as a perfect spin filter, such that in an FM configuration only 50% of the electrons at the Fermi surface of graphene can tunnel through it. Thus, in the AFM configuration one would expect zero tunnelling, because the two spin species are filtered by different layers. The actual degree of spin filtering will be less than 100%, leading to finite resistance even in the AFM state. In thicker CrI<sub>3</sub> layers, tunnelling has been shown to involve additional steps for out-of-plane fields but a smooth evolution for in-plane fields. Thus, tunnelling magnetoresistance (TMR) experiments have confirmed an AFM configuration between layers, with the moment along the  $c$  axis. Given the large TMR observed, these studies<sup>38–40</sup> have paved the way for the development of tunnelling-based memory, sensing and spin-filtering devices. Magnetic vdW materials are also expected to produce novel optoelectronic devices. Indeed, magnetic tuning of emission in heterostructures has already been observed<sup>13</sup> and predictions of electrical tuning of the Kerr effect have been reported<sup>49</sup>.

As in a wide variety of materials<sup>50–53</sup>, electric fields have been applied to manipulate the ordered phase in magnetic vdW materials. Many studies of CrI<sub>3</sub> have used structures with hBN spacers between the graphene layers and the CrI<sub>3</sub>, with an additional graphene layer in direct contact with the magnetic layer<sup>17,37</sup>. This allowed probing the magnetism via MCD while either the doping level or the electric field across the layer was tuned. As shown in Fig. 2, the MCD is hysteretic and shows jumps with respect to an electric field applied across the layers. Interestingly, similar effects have been observed with doping and have been attributed to switching that results from reducing the critical

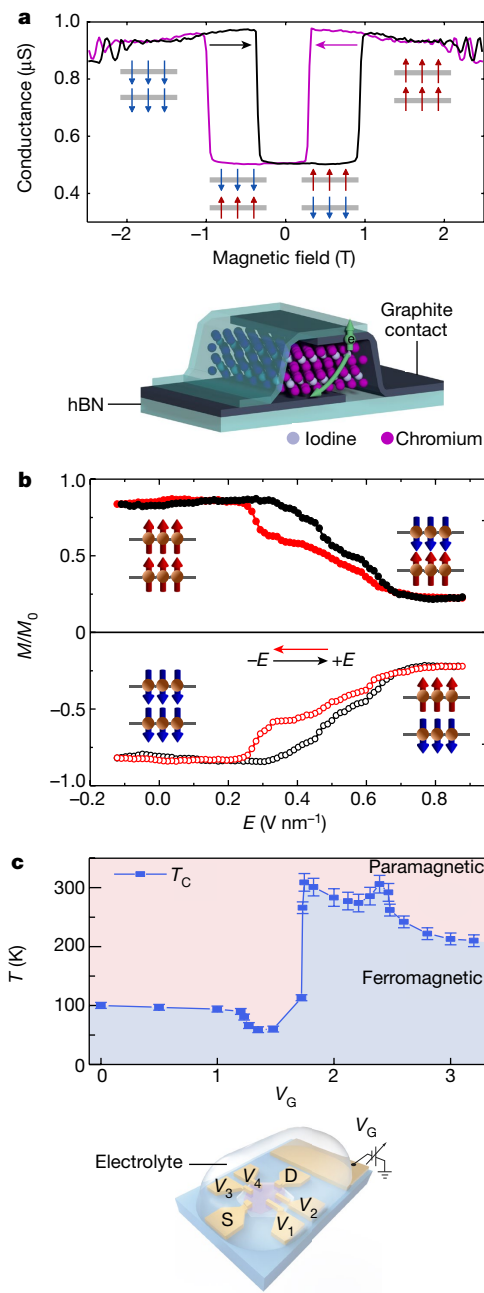


**Fig. 3 | Electrical measurements and tuning of 2D magnetism.**

**a**, Tunnelling between graphene layers spaced by  $\text{CrI}_3$  as a function of applied magnetic field and sweep direction (indicated by black and purple arrows). The device layout is shown in the inset and the magnetic configuration is shown by the red and blue arrows. The sudden increase in conductance is attributed to the enhanced net transmission that occurs when the two layers are aligned (bottom schematic; from ref. <sup>39</sup>). Reprinted with permission from AAAS.). **b**, MCD signal  $M$  of bilayer  $\text{CrI}_3$ , normalized by its saturation value  $M_0$ . The data were taken at 4 K with a magnetic field just above the critical value for the metamagnetic transition. Upon applying an electric field, the sample is tuned back to the AFM state<sup>37</sup>. Image reprinted with permission from ref. <sup>37</sup>, Springer Nature Limited. **c**, The ferromagnetic (blue) and paramagnetic (pink) of  $\text{Fe}_3\text{GeTe}_2$ , with the transition temperature measured using the anomalous Hall effect. The critical temperature  $T_c$  (blue points) is tuned by applying a gate voltage  $V_g$  through an ionic liquid (see bottom schematic; S, source; D, drain; four probes (V1, V2, V3, V4))<sup>30</sup>. Image reprinted from ref. <sup>30</sup>.

magnetic field for the metamagnetic transition. This suggests that the field across the layers results in doping across the device, such that the induced carriers mediate an enhanced ferromagnetic exchange<sup>37</sup>, consistent with studies of non-vdW materials<sup>34</sup>. Electrostatic gating

**Table 1 | List of potential research topics in four categories for magnetic van der Waals materials**

Research directions	Specific topics
New materials	Room-temperature ferromagnetic and antiferromagnetic materials Multiferroic materials Magnetic vdW materials with quantum spin ( $S = 1/2$ ) Magnetic vdW materials with $4d/5d$ elements and strong spin-orbit coupling Unconventional superconductors
Fundamental issues	Evolution of magnetic fluctuations as a function of layer number: Ising, XY and Heisenberg models XY model: BKT transition, vortex–antivortex pair fluctuations Effects of interface, including substrate and capping layer Proximity with other quantum phases: $s$ -, $p$ - and $d$ -wave superconductors, ferroelectrics, FMs, AFMs Spin–valley coupling Magnetic excitons
Devices and applications	Controllability via strain and gating Heterostructures Magnetic sensors Terahertz magneto-optical devices Multiferroics Spintronics Topological quantum computing
Quantum and topological phases	Quantum spin liquids Quantum critical phenomena induced by external variables Unconventional superconductivity in two dimensions Kitaev interaction, spin-liquid physics and fractionalization Quantum spin Hall effect Skyrmions Landscaping quantum phases

has also been applied to tune  $T_c$  in the vdW ferromagnetic semiconductors  $\text{Cr}_2\text{Ge}_2\text{Te}_6$ <sup>55,56</sup> and  $\text{Fe}_3\text{GeTe}_2$ <sup>30</sup>. In the latter, the use of an ionic liquid produced a  $T_c$  above room temperature. As shown in Fig. 3c, the dependence of the transition temperature on the gate voltage was highly non-monotonic, suggesting that the doping moved the Fermi level into a new band. However, because the Li ions were intercalated into  $\text{Fe}_3\text{GeTe}_2$ , disorder and strain effects may have also played a part. We anticipate that spectroscopic probes will be employed to uncover the origin of this enhancement, as well as comparison with the use of chemical doping of the initial bulk crystal to further enhance and tune  $T_c$ . This exciting development also holds promise for electrical control of magnetism in functional devices. From a fundamental perspective, we anticipate that electric fields and heterostructures applied to AFMs, topologically ordered materials and potential spin-liquid magnetic vdW materials will reveal novel superconducting states<sup>1</sup>.

## New quantum phases and outlook

Going forward, we believe that there are four main directions to be pursued in the study and use of magnetic vdW materials (see Table 1). The first is the discovery of new materials with specific functionality—for example, the recent development of magnetic 2D vdW materials with transition temperatures at or above room temperature<sup>24,25</sup>. Pushing  $T_c$  higher will be crucial for real applications and will simultaneously provide a wider range of possible probes and ground states, given the rather large exchange energies involved. One can envision further increasing  $T_c$  by optimizing two key parameters, the exchange interaction and the magnetic anisotropy, with the latter being crucial for suppressing fluctuations that destroy long-range order<sup>57</sup>. It will also be very interesting to speculate what will lie ahead once we synthesize systems with quantum spins or strong spin-orbit coupling—for example, materials with elements such as  $\text{Cu}^{2+}$  or  $4d/5d$  transition metals. These should provide materials with strong fluctuations or fractional excitations that can be exploited to potentially mediate novel unconventional superconductors in 2D materials and heterostructures. Key to these efforts will be the simultaneous enhancement of the exchange interaction and tuning of the magnetic anisotropy<sup>19,34</sup>.

The second direction involves using these new materials to deepen our understanding of quantum materials. Specifically, numerous phases emerge when multiple physical effects compete, and it is often difficult to tune a single parameter in a material without inadvertently affecting the others (for example, doping level and disorder). It is entirely conceivable to achieve a detailed measurement of spin fluctuations for the four fundamental Hamiltonians—of the Ising, XY, Heisenberg and Kitaev models—as a function of layer number and temperature, with any combination of external variables of interest. Thus, one can study in detail the spatial and temporal map of vortex–antivortex pair creation and annihilation for the XY model below and above its BKT transition. It is also plausible to examine how these fluctuations vary in proximity with other materials, such as substrates, capping layers and materials with their own order (for example, superconductors or ferroelectrics). Other challenging, yet entirely possible, aims include spin–valley coupling and the magnetic exciton.

The third direction concerns the implementation of these materials in novel devices and applications. By building on the works summarized in ‘Initial devices and electrical probes’, there is room for novel concepts, such as the synaptic memory effects found in CrPS<sub>4</sub><sup>58</sup>. For successful implementation in real devices, it is of the utmost importance to understand and exploit the control of the ground state via strain and gating. The fact that magnetic vdW materials are intrinsically 2D makes them much more amenable to external stimuli. In addition, heterostructures unachievable by other techniques (for example, twists, periodic strain or lattice-mismatched materials) can be straightforwardly combined. Another important—and perhaps far-reaching, if realized—application is the use of 2D magnetic vdW materials in spintronics<sup>13,18</sup>. The intrinsic atomic limit of these materials renders them excellent platforms for future applications, such as spin injection through half-metallicity.

Last, but not least, it is very exciting to speculate on how one can realize quantum and topological phases using these materials. We note that most magnetic vdW materials form with the magnetic elements in a honeycomb lattice. With strong spin–orbit coupling and two neighbouring magnetic ions sharing an edge bond, we expect a Kitaev directional exchange interaction. Therefore, many magnetic vdW materials are subject to the competition among the Kitaev, Heisenberg and anisotropic exchange terms<sup>59</sup>. This competition can in principle lead to exotic quantum spin liquids, revealing fractionalized, magnetic Majorana fermions in real materials<sup>2,32,43</sup>. There is also the potential to realize other topological phases and particles in magnetic systems, such as the quantum spin Hall effect<sup>60</sup> or skyrmions<sup>26</sup>. Other interesting opportunities include taking advantage of the intrinsically strong spin fluctuations to produce unconventional superconductivity by doping, proximity or pressure.

In the 2D limit, fluctuations—either quantum or classical—are typically very strong, which suggests the possible presence of new quantum phases in some nearby corners of the material parameter space. Clever implementation of heterostructures and perturbations should provide access to these phases without falling into nearby, sometimes trivial, alternative states. In essence, magnetic vdW materials offer us an entirely new opportunity to landscape quantum phases.

Received: 14 May 2018; Accepted: 20 August 2018;

Published online 31 October 2018.

- Lee, P. A. et al. Doping a Mott insulator: physics of high-temperature superconductivity. *Rev. Mod. Phys.* **78**, 17–85 (2006).
- Kitaev, A. Anyons in an exactly solved model and beyond. *Ann. Phys.* **321**, 2–111 (2006).
- Onsager, L. Crystal statistics. I. A two-dimensional model with an order–disorder transition. *Phys. Rev.* **65**, 117–149 (1944).
- Berezinskii, V. Destruction of long-range order in one-dimensional and two-dimensional systems having a continuous symmetry group I. Classical systems. *Sov. Phys. JETP* **32**, 493–500 (1971).
- Kosterlitz, J. M. & Thouless, D. J. Ordering, metastability and phase transitions in two-dimensional systems. *J. Phys. C* **6**, 1181–1203 (1973).
- Mermin, N. D. & Wagner, H. Absence of ferromagnetism or antiferromagnetism in one- or two-dimensional isotropic Heisenberg models. *Phys. Rev. Lett.* **17**, 1133–1136 (1966).
- Hellman, F. et al. Interface-induced phenomena in magnetism. *Rev. Mod. Phys.* **89**, 025006 (2017).
- Zak, J., Moog, E. R., Liu, C. & Bader, S. D. Universal approach to magneto-optics. *J. Magn. Magn. Mater.* **89**, 107–123 (1990).
- Arnold, C. S., Dunlavy, M. & Venus, D. Magnetic susceptibility measurements of ultrathin films using the surface magneto-optic Kerr effect: optimization of the signal-to-noise ratio. *Rev. Sci. Instrum.* **68**, 4212–4216 (1997).
- Elmers, H.-J. et al. Critical behavior of the uniaxial ferromagnetic monolayer Fe(110) on W(110). *Phys. Rev. B* **54**, 15224–15233 (1996).
- Park, J.-G. Opportunities and challenges of two-dimensional magnetic van der Waals materials: magnetic graphene? *J. Phys. Condens. Matter* **28**, 301001 (2016).

**This paper highlighted the importance of magnetic vdW materials and the huge potential of this new class of materials.**

- Roldán, R., Castellanos-Gómez, A., Cappelluti, E. & Guinea, F. Strain engineering in semiconducting two-dimensional crystals. *J. Phys. Condens. Matter* **27**, 313201 (2015).
- Zhong, D. et al. Van der Waals engineering of ferromagnetic semiconductor heterostructures for spin and valleytronics. *Sci. Adv.* **3**, e1603113 (2017).
- Cao, Y. et al. Unconventional superconductivity in magic-angle graphene superlattices. *Nature* **556**, 43–50 (2018).
- Busceme, M. et al. Photocurrent generation with two-dimensional van der Waals semiconductors. *Chem. Soc. Rev.* **44**, 3691–3718 (2015).
- Sachs, B. et al. Ferromagnetic two-dimensional crystals: single layers of K<sub>2</sub>CuF<sub>4</sub>. *Phys. Rev. B* **88**, 201402 (2013).
- Huang, B. et al. Electrical control of 2D magnetism in bilayer CrI<sub>3</sub>. *Nat. Nanotechnol.* (2018).

**This study demonstrated the controllability of 2D magnetism in the magnetic vdW material CrI<sub>3</sub>.**

- Samarth, N. Magnetism in flatland. *Nature* **546**, 216–218 (2017).
- Lado, J. L. & Fernández-Rossier, J. On the origin of magnetic anisotropy in two dimensional CrI<sub>3</sub>. *2D Mater.* **4**, 35002 (2017).
- Huang, B. et al. Layer-dependent ferromagnetism in a van der Waals crystal down to the monolayer limit. *Nature* **546**, 270–273 (2017).

**This study demonstrated the layer dependence of the ferromagnetic transition in the magnetic vdW material CrI<sub>3</sub> as a function of layer number.**

- Lee, J.-U. et al. Ising-type magnetic ordering in atomically thin FePS<sub>3</sub>. *Nano Lett.* **16**, 7433–7438 (2016).

**This work showed that one can exfoliate an atomically thin monolayer of the antiferromagnetic vdW material FePS<sub>3</sub> and demonstrated the Onsager solution for a real magnetic vdW material.**

- Wang, X. et al. Raman spectroscopy of atomically thin two-dimensional magnetic iron phosphorus trisulfide (FePS<sub>3</sub>) crystals. *2D Mater.* **3**, 31009 (2016).
- Gong, C. et al. Discovery of intrinsic ferromagnetism in two-dimensional van der Waals crystals. *Nature* **546**, 265–269 (2017).

**This study demonstrated the layer dependence of the ferromagnetic transition in the magnetic vdW material Cr<sub>2</sub>Ge<sub>2</sub>Te<sub>6</sub> as a function of layer number.**

- Bonilla, M. et al. Strong room-temperature ferromagnetism in VSe<sub>2</sub> monolayers on van der Waals substrates. *Nat. Nanotechnol.* **13**, 289–293 (2018).
- O’Hara, D. J. et al. Room temperature intrinsic ferromagnetism in epitaxial manganese selenide films in the monolayer limit. *Nano Lett.* **18**, 3125–3131 (2018).
- Mühlbauer, S. et al. Skyrmion lattice in a chiral magnet. *Science* **323**, 915–919 (2009).
- Geim, A. K. & Grigorieva, I. V. Van der Waals heterostructures. *Nature* **499**, 419–425 (2013).
- Williams, T. J. et al. Magnetic correlations in the quasi-2D semiconducting ferromagnet CrSiTe<sub>3</sub>. *Phys. Rev. B* **92**, 144404 (2015).
- Tian, Y., Gray, M. J., Ji, H., Cava, R. J. & Burch, K. S. Magneto-elastic coupling in a potential ferromagnetic 2D atomic crystal. *2D Mater.* **3**, 025035 (2016).
- Deng, Y. et al. Gate-tunable room-temperature ferromagnetism in two-dimensional Fe<sub>3</sub>GeTe<sub>2</sub>. Preprint at <https://arxiv.org/abs/1803.02038> (2018).
- Kuo, C. T. et al. Exfoliation and Raman spectroscopic fingerprint of few-layer NiPS<sub>3</sub> van der Waals crystals. *Sci. Rep.* **6**, 20904 (2016).
- Banerjee, A. et al. Neutron scattering in the proximate quantum spin liquid  $\alpha$ -RuCl<sub>3</sub>. *Science* **356**, 1055–1059 (2017).
- Plumb, K. W. et al.  $\alpha$ -RuCl<sub>3</sub>: a spin-orbit assisted Mott insulator on a honeycomb lattice. *Phys. Rev. B* **90**, 041112 (2014).
- Abramchuk, M. et al. Controlling magnetic and optical properties of the van der Waals crystal CrCl<sub>3</sub>- $\lambda$ Br<sub>x</sub> via mixed halide chemistry. *Adv. Mater.* <https://doi.org/10.1002/adma.201801325> (2018).
- Ando, K., Takahashi, K., Okuda, T. & Umehara, M. Magnetic circular dichroism of zinc-blende-phase MnTe. *Phys. Rev. B* **46**, 12289–12297 (1992).
- Lange, M. et al. A high-resolution combined scanning laser and widefield polarizing microscope for imaging at temperatures from 4 K to 300 K. *Rev. Sci. Instrum.* **88**, 123705 (2017).
- Jiang, S., Shan, J. & Mak, K. F. Electric-field switching of two-dimensional van der Waals magnets. *Nat. Mater.* **17**, 406–410 (2018).
- Song, T. et al. Giant tunnelling magnetoresistance in spin-filter van der Waals heterostructures. *Science* **360**, 1214–1218 (2018).
- Klein, D. R. et al. Probing magnetism in 2D van der Waals crystalline insulators via electron tunneling. *Science* **360**, 1218–1222 (2018).
- Kim, H. H. et al. One million percent tunnel magnetoresistance in a magnetic van der Waals heterostructure. *Nano Lett.* **18**, 4885–4890 (2018).
- Burch, K. S., Awschalom, D. D. & Basov, D. N. Optical properties of III-Mn-V ferromagnetic semiconductors. *J. Magn. Magn. Mater.* **320**, 3207–3228 (2008).

42. Sandilands, L. J. et al. Stability of exfoliated  $\text{Bi}_2\text{Sr}_2\text{Dy}_x\text{Ca}_{1-x}\text{Cu}_2\text{O}_{8+\delta}$  studied by Raman microscopy. *Phys. Rev. B* **82**, 064503 (2010).

43. Nasu, J., Knolle, J., Kovrizhin, D. L., Motome, Y. & Moessner, R. Fermionic response from fractionalization in an insulating two-dimensional magnet. *Nat. Phys.* **12**, 912–915 (2016).

44. Bozhko, D. A. et al. Supercurrent in a room-temperature Bose–Einstein magnon condensate. *Nat. Phys.* **12**, 1057–1062 (2016).

45. An, K. et al. Magnons and phonons optically driven out of local equilibrium in a magnetic insulator. *Phys. Rev. Lett.* **117**, 107202 (2016).

46. Wang, Z. K., Lim, H. S., Ng, S. C., Özylmaz, B. & Kuok, M. H. Brillouin scattering study of low-frequency bulk acoustic phonons in multilayer graphene. *Carbon* **46**, 2133–2136 (2008).

47. Worledge, D. C. & Geballe, T. H. Magnetoresistive double spin filter tunnel junction. *J. Appl. Phys.* **88**, 5277–5279 (2000).

48. Miao, G. X., Müller, M. & Moodera, J. S. Magnetoresistance in double spin filter tunnel junctions with nonmagnetic electrodes and its unconventional bias dependence. *Phys. Rev. Lett.* **102**, 076601 (2009).

49. Sivadas, N., Okamoto, S. & Xiao, D. Gate-controllable magneto-optic Kerr effect in layered collinear antiferromagnets. *Phys. Rev. Lett.* **117**, 267203 (2016).

50. Bollinger, A. T. et al. Superconductor–insulator transition in  $\text{La}_{2-x}\text{Sr}_x\text{CuO}_4$  at the pair quantum resistance. *Nature* **472**, 458–460 (2011).

51. Leng, X., Garcia-Barriocanal, J., Bose, S., Lee, Y. & Goldman, A. M. Electrostatic control of the evolution from a superconducting phase to an insulating phase in ultrathin  $\text{YBa}_2\text{Cu}_3\text{O}_{7-x}$  films. *Phys. Rev. Lett.* **107**, 027001 (2011).

52. Nojima, T. et al. Hole reduction and electron accumulation in  $\text{YBa}_2\text{Cu}_3\text{O}_y$  thin films using an electrochemical technique: evidence for an n-type metallic state. *Phys. Rev. B* **84**, 020502 (2011).

53. Ahn, C. H., Triscone, J.-M. & Mannhart, J. Electric field effect in correlated oxide systems. *Nature* **424**, 1015–1018 (2003).

54. Ahn, C. H. et al. Electrostatic modification of novel materials. *Rev. Mod. Phys.* **78**, 1185–1212 (2006).

55. Xing, W. et al. Electric field effect in multilayer  $\text{Cr}_2\text{Ge}_2\text{Te}_6$ : a ferromagnetic 2D material. *2D Mater.* **4**, 24009 (2017).

56. Chen, Y. et al. Role of oxygen in ionic liquid gating on two-dimensional  $\text{Cr}_2\text{Ge}_2\text{Te}_6$ : a non-oxide material. *ACS Appl. Mater. Inter.* **10**, 1383–1388 (2018).

57. Irkhin, V. Y. & Katanin, A. A. Kosterlitz–Thouless and magnetic transition temperatures in layered magnets with a weak easy-plane anisotropy. *Phys. Rev. B* **60**, 2990–2993 (1999).

58. Lee, M. J. et al. Synaptic devices implemented with two-dimensional layered single crystal chromium thiophosphate ( $\text{CrPS}_4$ ). *NPG Asia Mater.* **10**, 23–30 (2018).

59. Jackeli, G. & Khaliullin, G. Mott insulators in the strong spin–orbit coupling limit: from Heisenberg to a quantum compass and Kitaev models. *Phys. Rev. Lett.* **102**, 017205 (2009).

60. Lee, K. H., Chung, S. B., Park, K. & Park, J.-G. Magnonic quantum spin Hall state in the zigzag and stripe phases of the antiferromagnetic honeycomb lattice. *Phys. Rev. B* **97**, 180401 (2018).

**Acknowledgements** We acknowledge useful discussions with D. Xiao and X. Xu. K.S.B. was supported by the National Science Foundation through grant DMR-1709987 and D.M. acknowledges support from the National Science Foundation under grant DMR-1410428. J.-G.P. was supported by the Institute for Basic Science (IBS) of Korea (IBS-R009-G1).

**Reviewer information** *Nature* thanks M. Katsnelson and the other anonymous reviewer(s) for their contribution to the peer review of this work.

**Author contributions** J.-G.P. initiated the project and all authors wrote the manuscript.

**Competing interests** The authors declare no competing interests.

**Additional information**

**Reprints and permissions information** is available at <http://www.nature.com/reprints>.

**Correspondence and requests for materials** should be addressed to J.-G.P.

**Publisher's note:** Springer Nature remains neutral with regard to jurisdictional claims in published maps and institutional affiliations.